ELSEVIER

Journal of Applied Geophysics 47 (2001) 83–96

APPLIED GEOPHYSICS

www.elsevier.nl/locate/jappgeo

A rapid electrical sounding method The «three-point» method: a Bayesian approach

Henri Robain [a,*], Muriel Lajarthe [b], Nicolas Florsch [b]

[a] *IRD ORSTOM, Laboratoire de Geophysique 32 Avenue Henri Varagnat, F-93143 Bondy Cedex, France*
[b] *C.L.D.G., Université de La Rochelle, Avenue Marillac, 17042 La Rochelle Cedex 01, France*

Received 28 April 2000; accepted 19 April 2001

Abstract

Only three independent measurements of apparent resistivity are theoretically sufficient to retrieve the parameters of a geoelectrical model with two layers, i.e. the resistivities of the two layers and the thickness of the first one. The Three-Point Method (TPM) presented here is a rapid electrical sounding field procedure based on that principle. It consists of measuring the apparent resistivity using only three interelectrode spacings instead of some tens as for a usual vertical electrical sounding. To invert these data and check out the limits of this simplified field procedure, we use a Bayesian probabilistic formalism. Such an approach appears more effective than other traditional inversion methods because it allows to calculate exhaustively a probabilistic description of the equivalent solutions. Both synthetic and field data validate TPM when a model with two layers correctly describes the geoelectrical structure of the ground. Particularly, TPM combined with the Bayesian inversion method is a tool well-designed to rapidly characterise the overburden thickness in sedimentary contexts, or the water table depth in the case of sufficient resistivity contrast between saturated and nonsaturated materials.

Keywords: DC resistivity; Vertical electrical sounding; Rapid field procedure; Bayesian inversion

1. Introduction

In electrical prospecting, three main approaches are commonly used to investigate ground resistivities from surface measurements.

• Apparent resistivity maps, which are obtained by moving a constant array along a regular mesh. They provide qualitative information about resistivity lateral variations in the range of the investigation depth of the used array (Roy and Apparao, 1971). Such maps are frequently used for archaeological or civil engineering studies that principally aim at delineating buried structures such as roads, moats, walls, pipes or waste deposits (Scollar et al., 1990).

• Vertical Electrical Soundings (usually abbreviated as VES), which are obtained by increasing the array size (i.e., the depth of investigation) at a given location. VES apparent resistivity data are then processed with inversion algorithms to retrieve quantitative information about the geoelectrical layering below the sounding centre (i.e., resistivities and thicknesses of the different layers). Such soundings are widely used for underground water prospecting or mining surveys (Telford et al., 1990). It should be

* Corresponding author. Tel.: +33-1-4802-5636; fax: +33-1-4847-3088.
E-mail address: Henri.Robain@bondy.ird.fr (H. Robain).

0926-9851/01/$ - see front matter
PII: S0926-9851(01)00049-0

pointed out that the classical 1D inversion of VES data supposes that the structure of the ground is almost tabular. It is clear that in some cases, this hypothesis is not realistic and hence troublesome. In such cases, at least 2D, and better still 3D, surveys and inversion processes are required.

- Electrical pseudosections (also called 2D electrical imaging) is another method widely used for mining surveys. It has been recently adapted to environmental investigations since computer-controlled resistivity meters are allowed to efficiently perform hundreds of measurements sweeping any combination of four electrodes among several tens implanted in line (Griffiths and Turnbull, 1985; Griffiths et al., 1990). The pseudosection is then processed using 2D inversion algorithms—finite differences or finite elements—to retrieve a smooth model of resistivity variations as a function of depth along the surveyed line (Barker, 1992; Griffiths and Barker, 1993; Lokhe and Barker, 1996a).

At present, there is an increasing demand for 3D investigations (Dabas et al., 1994; Sasaki, 1994; Zhang et al., 1995; Lokhe and Barker, 1996b), and even for 3D plus time investigations. The repetition of electrical soundings according to a regular grid (Robain et al., 1996) or the implementation of close parallel pseudosections (Park, 1998; Chambers et al., 1999) may provide reliable 3D information. However, such surveys remain strenuous and require a lot of time. Consequently, they are costly and moreover, not suitable when a short time lapses between the successive surveys is required for environmental monitoring, e.g. groundwater movement or contaminants diffusion. For such studies, there is still a considerable requirement for rapid methods, which could allow the survey of a site at least within a few days.

In environmental and more particularly in hydrological studies where water table depth is usually looked for, a simplification of ground structure into a two-layer model is often relevant. The unsaturated zone above the groundwater table is resistive while the saturated zone beneath is conductive. For this kind of simplified two-layer model, it is theoretically possible to retrieve two resistivities and one thickness (i.e., three parameters: r_1, r_2 and h) from only three independent measurements of apparent resistivity. One can then consider the development of a rapid electrical sounding method. We call such a procedure as the Three-Point Method (TPM). This paper aims at assessing its reliability and its limitations.

2. Theory

To assess TPM, a simple modelling method of considering two parallel, isotropic and homogeneous layers is used (Bhattacharya and Patra, 1968). For a Wenner array, the apparent resistivity, noted as ρ (Ω m), may be written as an analytical series derived from the images method:

$$\rho = r_1\left(1+2\left(\sum_{i=1}^{+\infty}\left(\frac{r_2-r_1}{r_2+r_1}\right)^i \times\left(\frac{L}{\sqrt{\left(\frac{L}{2}\right)^2+i^2}}-\frac{L}{\sqrt{L^2+i^2}}\right)\right)\right)$$

$$\text{with } L=\frac{a}{h} \qquad (1)$$

where r_1 and r_2 are the resistivities of the first and second layers (Ω m), h is the thickness of the first layer (m), a is the interelectrode spacing of the Wenner array (m). NB: for a two-layer model, the thickness of the second layer is infinite.

With three measurements of apparent resistivity (noted as ρ_1, ρ_2 and ρ_3) relative to three different values of the parameter a (noted as a_1, a_2 and a_3), Eq. (1) gives a system with three equations containing the three unknown quantities (r_1, r_2 and h):

$$\rho_i = f(r_1, r_2, h, a_i) \qquad \text{with } i = 1 \cdots 3 \qquad (2)$$

As long as the three equations are independent, the resolution of such a system is theoretically possible. Hence, only three measurements of apparent resistivity (ρ_1, ρ_2 and ρ_3) corresponding to three different interelectrode spacings (a_1, a_2 and a_3) are

necessary to calculate the three parameters describing a geoelectrical model with two layers (r_1, r_2 and h).

However, it should already be pointed out that the choice of the three interelectrode spacings has a prominent influence on the reliability of the result. For example, if a_1, a_2 and a_3 are chosen to be too close to one another, it intuitively appears that the result will not be very consistent. In this case, many sounding curves and then many equivalent models may fit the three measurements points. Hence, to retrieve a reliable solution, the three apparent resistivities (ρ_1, ρ_2 and ρ_3) have to be sampled as well as possible the sounding curve. A geometrical increase of the interelectrode spacing, as shown in Eq. (3), is relevant to achieve this purpose (Fig. 1):

$$a_i = a_0 k^{i-2} \qquad \text{with } i = 1 \cdots 3 \tag{3}$$

where a_0 is a reference value (m) and k is a factor larger than 1 (dimensionless).

With such a relation linking a_1, a_2 and a_3, the determination of parameters a_0 and k is sufficient to discuss the best choice to reliably calculate the model parameters (r_1, r_2 and h) from three apparent resistivity values. Considering Fig. 2, it appears that:

- a_0 has to be chosen close to the inflexion point of the electrical sounding curve. Actually, a_0 takes account of the interface depth. Hence, too small or too large values result to a poor estimation of the interface depth.
- k has to be chosen so that the two outer apparent resistivity values reach the steady tips of the sounding curve. Actually, k depends on the resistivity ratio r_2/r_1. When this ratio is high, the difference between the two tips of the sounding curve as well as the slope of the central part are high and vice versa. Hence, too small k values result to a poor estimation of this ratio.

2.1. Analysis of TPM reliability

Several methods may be used to calculate the parameters of a two-layer model (r_1, r_2 and h) from three apparent resistivity values:

- Any analytical method providing the resolution of the system, Eq. (2), which is a nonlinear system with three equations and three unknown quantities, for example, the Newton–Raphson scheme (Press et al., 1996).
- Any inversion algorithm of a vertical electrical sounding curve calculating the best fitting model. (e.g., Koefed, 1979).

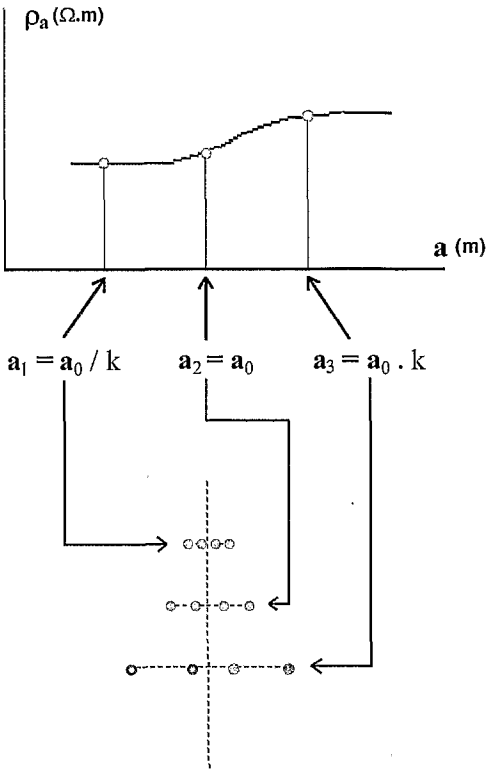

Fig. 1. Principle of the TPM (example with $a_0 = 1$ and $k = 2$).

Any of these methods provide values for the sought parameters, but it appears that there are generally many possible solutions. Particularly, the result strongly depends on the values given to initialise the iterative process. This uncertainty is more pronounced when the choice of the parameters a_0 and k is unfavourable.

This is illustrated on Fig. 3. Two models obtained with an inversion algorithm belonging to the second group of methods are presented. The difference between the inversion results only depends on the values given at the beginning of the iterative process. It clearly appears that only proper values for a_0 and k provides close models (Fig. 3a). Hence, in this favourable case, the result does not depend signifi-

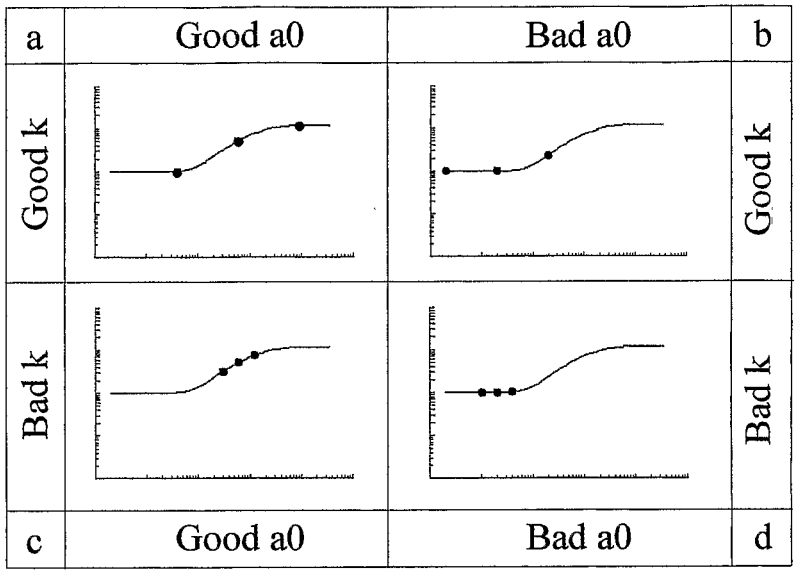

Fig. 2. Possible choices for a_0 and k parameters and the resulting sampling of the complete electrical sounding curve.

cantly on initialising values. For all the other cases, unfavourable a_0 and/or k, the calculated models are very different. With good a_0 and bad k, there is a strong indetermination for r_1 and h (Fig. 3b). With bad a_0 and good k, the indetermination mostly concerns r_2 (Fig. 3c). The highest indetermination is of course obtained with bad a_0 and bad k, but here it seems to mostly concern r_2 and h (Fig. 3d).

These examples clearly show that to reach reliable results with TPM, it is necessary to carefully choose a_0 and k. Practically:

- a_0 value must be approximately equal to twice the depth of the interface so that the median depth of investigation of the second array with spacing $a_2 = a_0$ is similar to the interface depth. For the Wenner array, the median depth of investigation is approximately half the interelectrode spacing (Edwards, 1977).
- k value must not be chosen too large because the first array with spacing $a_1 = a_0/k$ will then be sensitive to small near-surface inhomogeneities, which may violate the assumption of the two-layer model. From another point of view, the implementation of a very large third array with spacing $a_3 = a_0 k$ may be unsuited for an efficient field survey.

Hence, a priori values of thickness and resistivity ratio should be considered using some preliminary complete soundings to determine representative values of the three parameters (r_1, r_2 and h). A compromise has then to be found for the values of a_0 and k, which should, on one hand, bring a good description of the representative electrical sounding curve and, on the other hand, allow an efficient field survey.

Those preliminary complete soundings are also required to establish that a two-layer model is suitable. It particularly appears, as already pointed out, that TPM should be restricted to specific contexts where the consideration of only two layers is sufficient, e.g. the distinction between resistive unsaturated materials overlaying conductive saturated materials. Another important point is to establish that the depth of the interface does not vary greatly. Actually, the slope of the interface must be less than 10% in order to recover reliable interpretations using a 1D inversion process (Kunetz, 1966). If the slope is higher than 10% the TPM method, as any 1D method, should not be used.

2.2. Optimization of TPM: a Bayesian approach

Section 2.1 illustrates some equivalence ambiguities obtained with a classical inversion method but

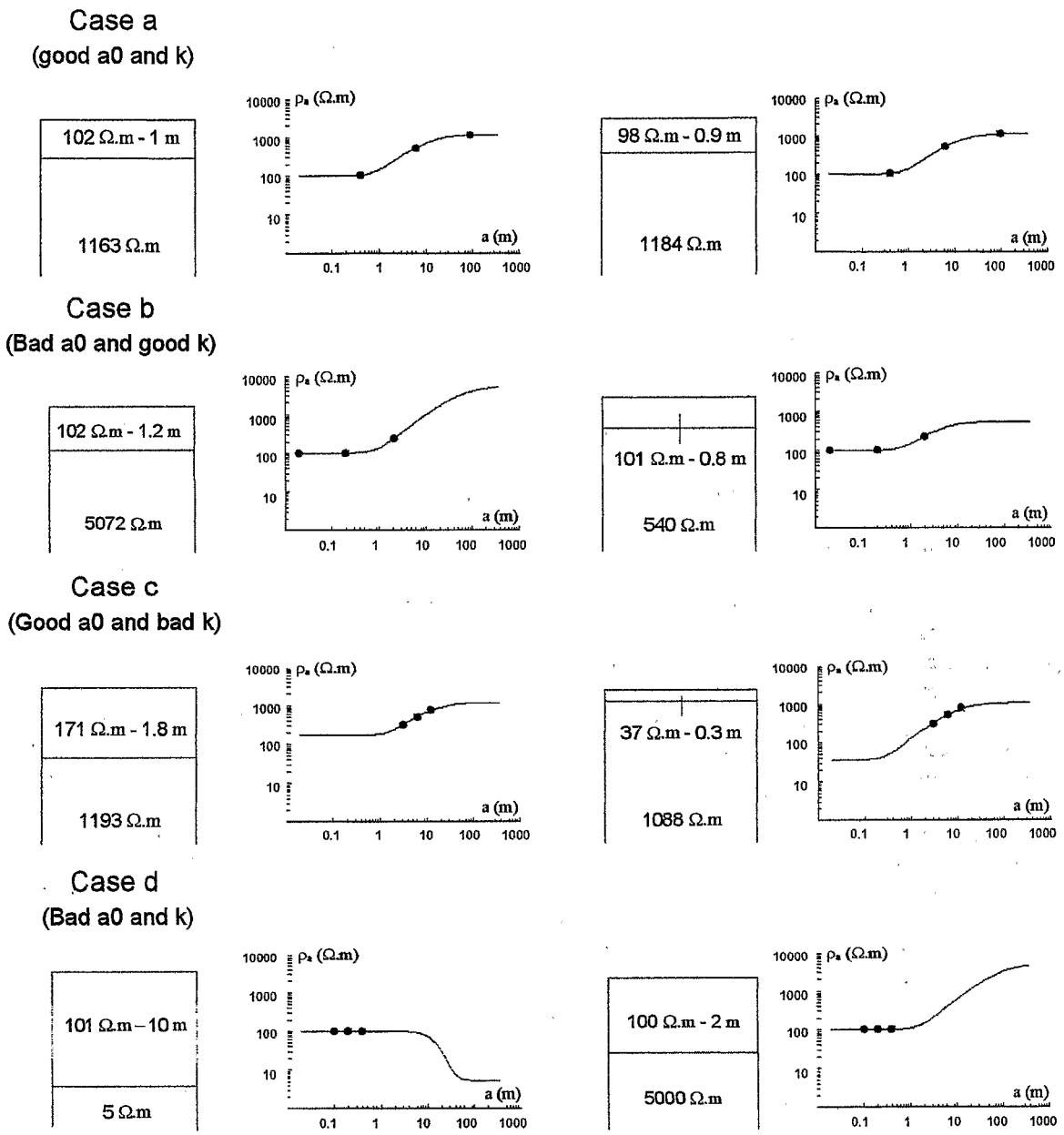

Fig. 3. Two different results obtained with TPM data and traditional inversion method (electrical sounding adjustment program). The apparent resistivities are extracted from the same synthetic two-layer curve ($\rho_1 = 100$ Ω m, $h = 1$ m and $\rho_2 = 1200$ Ω m) with $a_0 = 6$ and $k = 15$ (a), $a_0 = 0.2$ and $k = 15$ (b), $a_0 = 0.2$ and $k = 2$ (c) and $a_0 = 6$ and $k = 2$ (d). The difference between the two results is obtained only using different values to initiate the iterative process of inversion.

such algorithms are not designed to perform the exhaustive calculations needed to check the relevancy of the chosen TPM parameters (a_0 and k). A Bayesian probabilistic inversion approach appears more suitable for this purpose. This procedure consists of propagating the information available in data, expressed as a probability law, toward the parameter space through the linking physical law (Tarantola

and Valette, 1982a; Tarentola, 1987). The result obtained is the parameter probability density function (PDF), which provides a probabilistic description of all the possible solutions. The inverse problem solution can be defined as:

$$\sigma_p(\boldsymbol{p}) = \int \frac{\rho(\boldsymbol{d},\boldsymbol{p}) \cdot \theta(\boldsymbol{d},\boldsymbol{p})}{\mu(\boldsymbol{d},\boldsymbol{p})} \mathrm{d}\boldsymbol{d} \quad (4)$$

where $\boldsymbol{p}$ is the parameter vector; $\boldsymbol{d}$ is the data vector; $\sigma_p(\boldsymbol{p})$ is the a posteriori PDF for $\boldsymbol{p}$; $\rho(\boldsymbol{d},\boldsymbol{p})$ is the a priori PDF for $\boldsymbol{d}$ and $\boldsymbol{p}$; $\theta(\boldsymbol{d},\boldsymbol{p})$ is the PDF describing through physical laws the link between $\boldsymbol{d}$ and $\boldsymbol{p}$; $\mu(\boldsymbol{d},\boldsymbol{p})$ is the null information on $\boldsymbol{d}$ and $\boldsymbol{p}$.

Here, the parameter vector $\boldsymbol{p}$ consists of the two resistivities and the thickness describing the model (r_1, r_2, and h), and the data vector $\boldsymbol{d}$ consists of the three measured apparent resistivities (ρ_1, ρ_2 and ρ_3).

From this point, some legitimate hypothesis may be assumed:

- The null information is fixed to a constant value. Using the least square criterion to solve the inverse problem, Eq. (4), Tarantola and Valette (1982b) propose to define the null information imposing its stability with respect to a relevant group transformation. For a positive quantity x, a suitable form is described as follows:

$$\mu(x) = \frac{C}{x} \quad (5)$$

where C is a constant value.

Such a form corresponds to a Galilean transform. In electrical prospecting, we can restrict the Galilean transform to a simple scale transform. Consequently, the parameterization should be invariant by scale transform. It is easy to demonstrate that using $\log(x)$ instead of x, the null information becomes:

$$\tilde{\mu}(\log(x)) = \tilde{C} \quad (6)$$

Eq. (6) permits the invariance through a scale transformation. Hence, by using $\log(x)$ instead of x, the null information appearing in Eq. (4) is implicitly included in the following equation:

$$\sigma_p(\tilde{\boldsymbol{p}}) = \int \rho(\tilde{\boldsymbol{d}},\tilde{\boldsymbol{p}}) \cdot \theta(\tilde{\boldsymbol{d}},\tilde{\boldsymbol{p}}) \mathrm{d}\boldsymbol{d} \quad (7)$$

where $\tilde{\boldsymbol{p}}$ is the logarithm of parameter vector; $\tilde{\boldsymbol{d}}$ is the logarithm of data vector; $\sigma_p(\tilde{\boldsymbol{p}})$ is the a posteriori PDF for $\tilde{\boldsymbol{p}}$; $\rho(\tilde{\boldsymbol{d}},\tilde{\boldsymbol{p}})$ is the a priori PDF for $\tilde{\boldsymbol{d}}$ and $\tilde{\boldsymbol{p}}$; $\theta(\tilde{\boldsymbol{d}},\tilde{\boldsymbol{p}})$ is the PDF describing through physical laws the link between $\tilde{\boldsymbol{d}}$ and $\tilde{\boldsymbol{p}}$.

- We suppose that an equation linking data and parameters exits. Such an equation can be written as:

$$\boldsymbol{d} = G(\boldsymbol{p}) \quad (8)$$

where $\boldsymbol{d}$ is the data vector (measured apparent resistivities: ρ_1, ρ_2 and ρ_3), $\boldsymbol{p}$ is the parameters vector to be determined (resistivities r_1, r_2 and thickness h).

- We suppose that Eq. (8) is exact. In other words, we suppose that the two-layer model is suitable to describe the geoelectrical structure of the ground. This leads to Eq. (9) for PDF describing the physical links between data and parameters:

$$\theta(\boldsymbol{d},\boldsymbol{p}) = \delta(\boldsymbol{d} - G(\boldsymbol{p})) \quad (9)$$

where δ is a Dirac distribution.

- We suppose that data and parameters are independent. Hence, the joint a priori PDF for $\boldsymbol{d}$ and $\boldsymbol{p}$ may be derived as follows:

$$\rho(\boldsymbol{d},\boldsymbol{p}) = \rho_d(\boldsymbol{d}) \cdot \rho_p(\boldsymbol{p}) \quad (10)$$

This can be assumed if the survey itself does not influence the resistivity distribution in the ground. In the case of DC survey, it is clear that the injection of current in the ground does not modify its resistivity. From another point of view, the introduction of small conductive bodies in the ground (the electrodes) has no significant influence and hence may be neglected.

- The a priori PDF for each data is independent. This can be expressed with the data covariance matrix, which is a diagonal matrix in this case. We also suppose that the a priori PDF for each data follows a Gaussian law.

- For a given interval, the a priori PDF for parameters is set to a constant value. This corresponds to no a priori information concerning the PDF for parameters with the exception of the two values delineating the chosen interval.

With the previous hypothesis, the a posteriori PDF for parameters may be written as follows:

$$\sigma_p(\tilde{\boldsymbol{p}}) = \sigma_p(\tilde{r}_1,\tilde{r}_2,\tilde{h}) = k \exp\left[-\frac{1}{2}\sum_{i=1}^{3}\left(\frac{\tilde{v}_i - \tilde{\rho}_i}{\tilde{s}_i}\right)^2\right] \quad (11)$$

where k is a normalization factor (the probability full integral is equal to 1); $\tilde{s}_i$ is the standard deviation of the logarithm of the data; $\tilde{v}_i$ is the logarithm of the apparent resistivity calculated with the model (r_1, r_2, h); $\tilde{\rho}_i$ is the logarithm of the measured apparent resistivity.

Finally, the solution is given for r_1, r_2 and h as the PDF: $\sigma_p(\tilde{r}_1, \tilde{r}_2, \tilde{h})$. The probability for $\tilde{r}_1$ to belong to the interval $[\alpha_1, \beta_1]$, $\tilde{r}_2$ to belong to the interval $[\alpha_2, \beta_2]$, and $\tilde{h}$ to belong to the interval $[\alpha_3, \beta_3]$, is expressed by the following integration:

$$\sigma_p\left(\tilde{r}_1 \in [\alpha_1,\alpha_2]; \tilde{r}_2 \in [\alpha_2,\beta_2]; \tilde{h} \in [\alpha_3,\beta_3]\right) = \int_{\alpha_1}^{\beta_1}\int_{\alpha_2}^{\beta_2}\int_{\alpha_3}^{\beta_3}\sigma_p\left(\tilde{r}_1,\tilde{r}_2,\tilde{h}_1\right)\mathrm{d}\tilde{r}_1\mathrm{d}\tilde{r}_2\mathrm{d}\tilde{h} \quad (12)$$

It is not easy to give satisfying representations of three-dimensional functions like the one presented in Eq. (12). Hence, it seems preferable to draw separately the following three two-dimensional joint laws (computation details can be found in Florsch and Hinderer, 2000):

$$\sigma_{1,2}\left(\tilde{r}_1,\tilde{r}_2\right) = \int_{-\infty}^{+\infty}\sigma_p\left(\tilde{r}_1,\tilde{r}_2,\tilde{h}\right)\mathrm{d}\tilde{h} \quad (13.1)$$

$$\sigma_{1,3}\left(\tilde{r}_1,\tilde{h}\right) = \int_{-\infty}^{+\infty}\sigma_p\left(\tilde{r}_1,\tilde{r}_2,\tilde{h}\right)\mathrm{d}\tilde{r}_2 \quad (13.2)$$

$$\sigma_{2,3}\left(\tilde{r}_2,\tilde{h}\right) = \int_{-\infty}^{+\infty}\sigma_p\left(\tilde{r}_1,\tilde{r}_2,\tilde{h}\right)\mathrm{d}\tilde{r}_1 \quad (13.3)$$

These functions provide all the possible solutions and finally reveal the complete possible range. The more concentrated the density, the less important the variation domain of parameters. On the contrary, a spread density indicates that the corresponding parameters are not well-determined. The imaging of the Bayesian solution also allows to verify that the parameters a_0 and k have been correctly chosen.

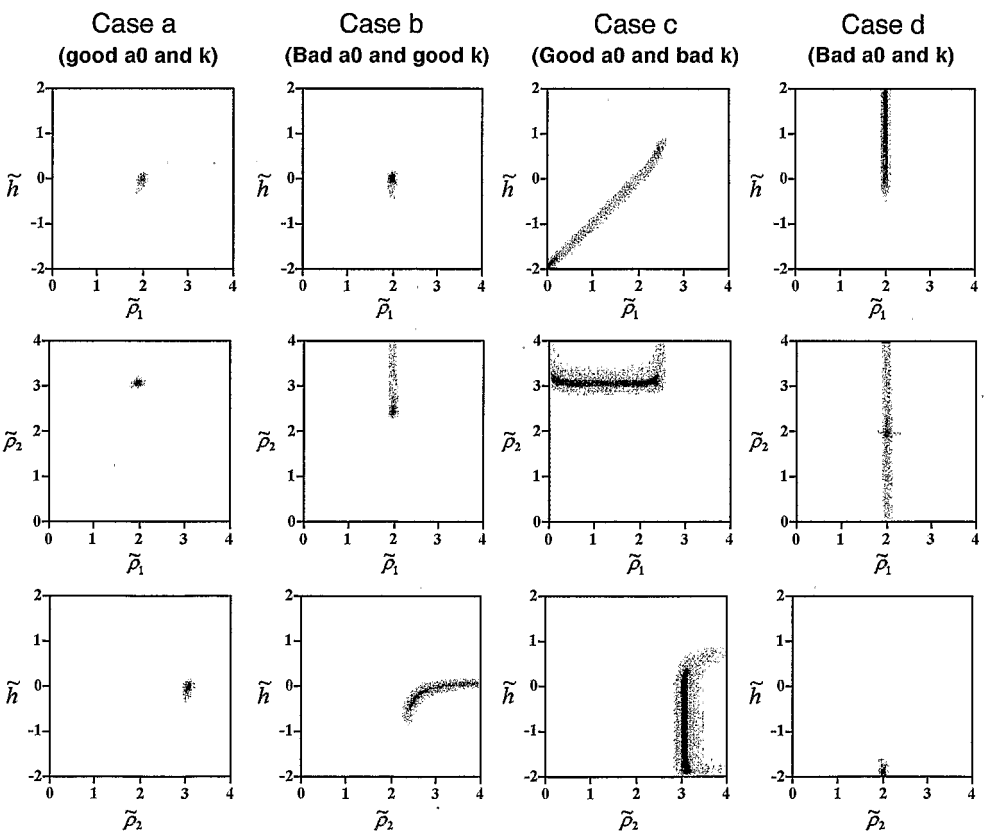

Fig. 4. Results of Bayesian inversion for the same data as in Fig. 3. Representation of the three marginal probability densities: log(ρ_1) versus log(h) (top), log(ρ_1) versus log(ρ_2) (centre) and log(ρ_2) versus log(h) (bottom).

Fig. 4 shows the results obtained by the Bayesian inversion for the apparent resistivity values processed with the classical inversion method (cf. Fig. 3).

The uncertainties shown on Fig. 3 are here exhaustively quantified. For case A (good a_0 and k), the probability density is concentrated around three particular values: $\log(r_1) = 2$ ($r_1 = 100$ Ω m), $\log(h) = 0$ ($h = 1$ m) and $\log(r_2) = 3.1$ ($r_2 = 1200$ Ω m). For cases B, C and D, the extent of probability densities brings an exhaustive quantification of equivalents model. For example, for case C (bad a_0 and k), r_1 is well-defined (100 Ω m), but h may take any value between 0.25 and 100 m while r_2 is completely undetermined.

3. Field examples

Two field examples are presented to validate TPM plus Bayesian inversion approach. The first example corresponds to sedimentary overburdens that can be modeled by a conductive layer (clayey materials) over a resistive one (limestone). The second example corresponds to very thick tropical weathering cover that can generally be modeled for the investigated depth by a resistive layer (nonsaturated materials) over a conductive one (groundwater).

It should be underlined that the aim of the case histories presented here is only to discuss the reliability of TPM approach and not to bring a complete description for the geoelectrical structure of the surveyed sites.

3.1. Conductive / resistive model (St. Agnant)

The first case history corresponds to the survey of a site located close to Saint Agnant locality (France). The thickness of the overburden ranges from a few decimeters to about 2 m.

First of all, a set of 10 complete electrical soundings has been performed with Wenner array (Fig. 5). The sounding curves were then interpreted by assuming a two-layer model. This preliminary survey shows that the overburden thickness is about 1 m and that the ratio r_2/r_1 does not exceed 10. In this case, the best TMP parameters may be fixed as follows: $a_0 = 2$ and $k = 15$ (or $a_1 = 0.13$ m, $a_2 = 2$ m and $a_3 = 30$ m).

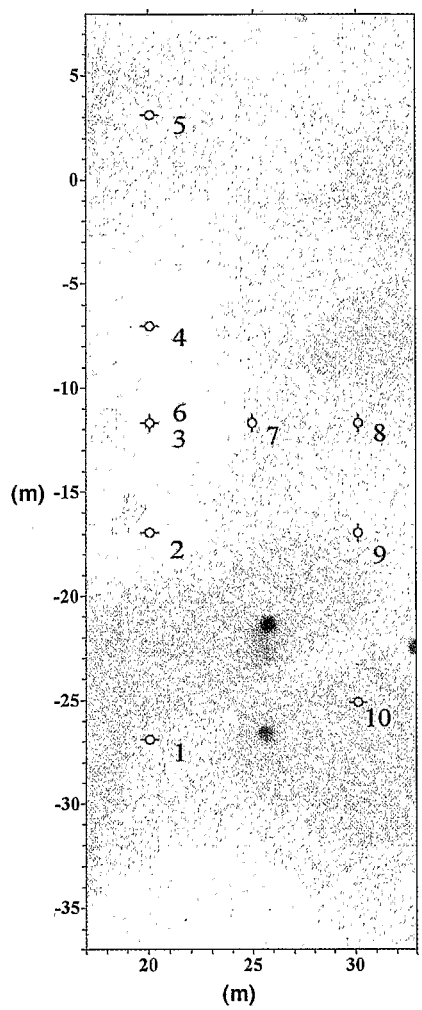

Fig. 5. Saint Agnant site: position of the detailed sounding over a pole–pole apparent resistivity map (AM = 0.5 m, grid = 0.5 × 0.5 m).

Fig. 6 shows the interpretation of the complete sounding no. 1 using a classical inversion algorithm. The result shows that $r_1 = 48$ Ω m, $h = 0.4$ m and $r_2 = 503$ Ω m. From the synthetic curve fitting the field data, TPM apparent resistivities corresponding to $a_0 = 2$ and $k = 15$ are extracted. A measurement noise corresponding to 5% standard deviation is added. Then, the Bayesian inversion is performed. In that case, probability densities are rather concentrated spots: r_1 ranges from 30 to 60 Ω m, r_2 from 400 to 600 Ω m, and h from 30 to 60 cm.

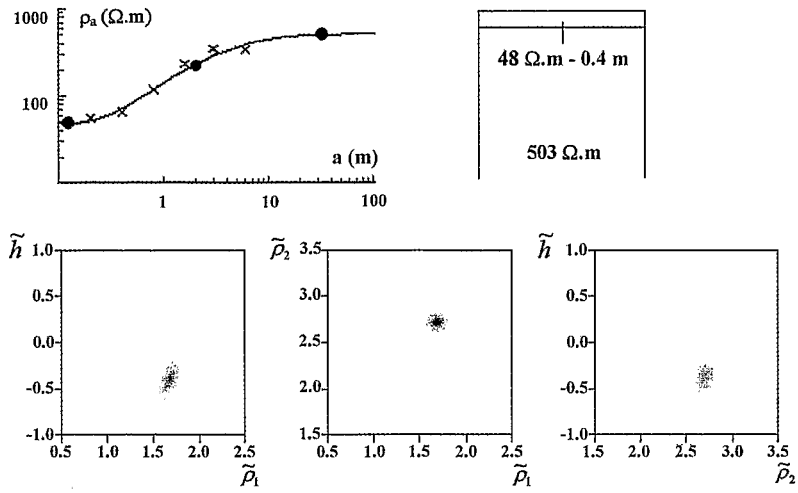

Fig. 6. Saint Agnant sounding no. 1: adjustment of the measurements by a traditional inversion method (left top); boxed diagram representing the traditional inversion result (right top); results of Bayesian inversion using three apparent resistivity extracted from the the adjusted curve with $a_0 = 2$ and $k = 15$, with a measurement noise of 5% standard deviation added (bottom).

Nevertheless, it is not easy in practice to implement TPM with these optimal parameters. For $a = 30$ m, the total extent of the Wenner array is 90 m. The implementation of such a long array over a fine mesh is often problematic. On the contrary, very small array such as $a = 0.15$ m is also troublesome for theoretical reasons. The definition of apparent resistivity actually supposes that current and potential electrodes can be regarded as joint electrodes at the surface of the ground. In the case of a very small array, the depth of electrode implantation may not be neglected with respect to the array extent, and so the measurements performed do not fulfill theoretical requirements. Hence, we decided to use a lower value for k ($k = 5$), which is a satisfying compromise between relevant description of the sounding curve and efficient implementation of TPM.

The same process as the one shown in Fig. 6 was undertaken for each complete sounding but with TPM parameters $a_0 = 2$ and $k = 5$ ($a_1 = 0.4$ m, $a_2 = 2$ m, and $a_3 = 10$ m).

The results were separated into two groups: the first one is represented by sounding no. 1, representative of sounding nos. 5, 8, 9 and 10 (Fig. 7a), and the second one by sounding no. 2, representative of sounding nos. 3, 4, 6 and 7 (Fig. 7b).

Contrary to Fig. 6, the probability density functions are not concentrated spots but elongated stains, showing rather poor determinations for r_2 in sounding no. 2 and both h and r_1 in sounding no. 1.

The first group of soundings corresponds to an area were the overburden thickness is small (cf. Fig. 5—high resistivity areas). The parameter a_0 is not well-adapted. Actually, it was chosen according to a larger mean h value. The three measurement points are shifted to the right end of the sounding curve. Hence, there is a low uncertainty for r_2. On the contrary, since k is rather small, the poor sampling of the left end of curve does not permit us to determine r_1 accurately. Consequently, there is also a wide range for thickness h because models with a constant ratio r_1/h are equivalent.

The second group of soundings corresponds to an area where the limestone lies at about 2 m depth (cf. Fig. 5). The chosen a_0 value is suitable for this thickness of the overburden. Hence, h and r_1 are well determined. On the contrary, the small k value does not permit us to sample the right end of the sounding curve. This explains the lack of accuracy for r_2 determination.

3.2. Resistive / conductive model (Nsimi)

The second case history corresponds to the survey of a site located close to Nsimi village (Cameroon)

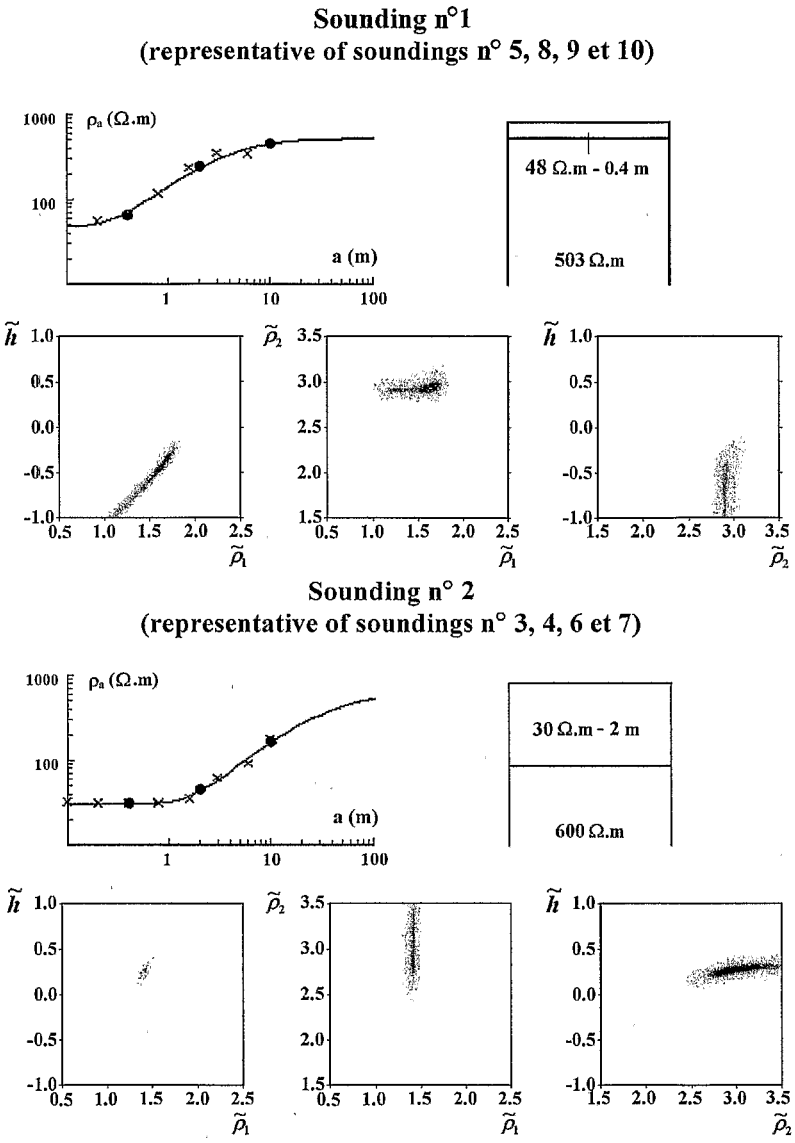

Fig. 7. Saint Agnant sounding nos. 1 and 2: adjustment of the measurements by a traditional inversion method (left top); boxed diagram representing the traditional inversion result (right top); results of Bayesian inversion using three apparent resistivity extracted from the the adjusted curve with $a_0 = 2$ and $k = 5$, with a measurement noise of 5% standard deviation added (bottom).

in the tropical rain forest. This site presents a typical lateritic weathered cover with, from top to bottom: clayey materials, pebbly materials indurated by iron oxyhydroxides and loamy materials. The total thickness of these materials varies a lot from point to point: the depth of the granitic basement ranges from 0 (outcrops) 40 m. The most frequent depth is about 25 m. The groundwater table generally lies within the loamy materials at depth varying from 15 m at the top of hill to 0 m in the swamp at the bottom of the hill. This site has been widely studied by the Institut de Recherche pour le Développement (IRD) to characterise the time evolution of both surface and ground waters and its interaction with the different

solid materials (Viers et al., 1997; Olivié-Lauquet et al., 1999; Olivia et al., 1999).

Numerous electrical measurements have been acquired on this site (Robain et al., 1995, 1998; Ritz et al., 1999). Particularly, a monthly electrical monitoring has been undertaken using a Wenner array with three different interelectrode spacings: $a = 10$, 20 and 40 m ($a_0 = 20$ m and $k = 2$). With such spacings, the penetration depth is generally compatible with two-layer models, which separate the resistive unsaturated material above the groundwater table from the conductive saturated materials beneath. Obviously, this is not proper for swampy areas where the suitable model should be very conductive/less conductive and moreover, for outcrop areas where the proper model should be a three-layer model resistive/conductive/resistive. In this last case, it is clear that TPM is not suitable. A "five-point method" should be developed to retrieve three resistivities and two thicknesses of such a three-layer model. From a

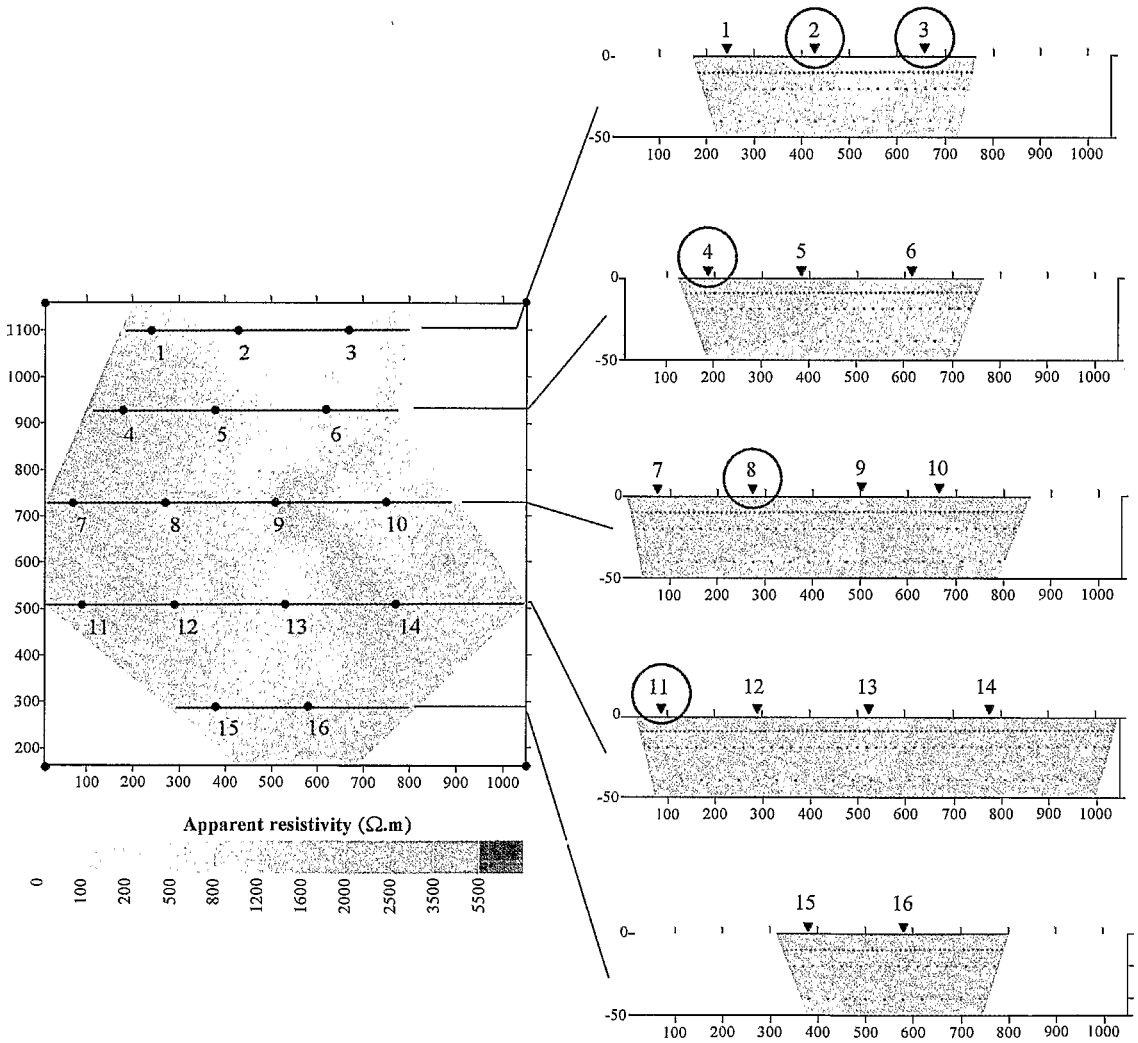

Fig. 8. Nsimi site: positions of the extracted soundings on a Wenner apparent resistivity map ($a = 10$ m) (left); positions of the extracted soundings along the simplified pseudosections obtained from the three Wenner profiling ($a = 10$, 20 and 40 m): dark grey: resistive (> 800 Ω m), grey: conductive (800–80 Ω m) and light grey: very conductive (< 80 Ω m) (right).

computational point of view, such a method needs to calculate an expression similar to Eq. (12) by scanning all the possible parameters on a given mesh. For a set of five parameters defined on a coarse grid (10×10), this leads to 10^{10} computations. The time required for such a process, even on a very powerful

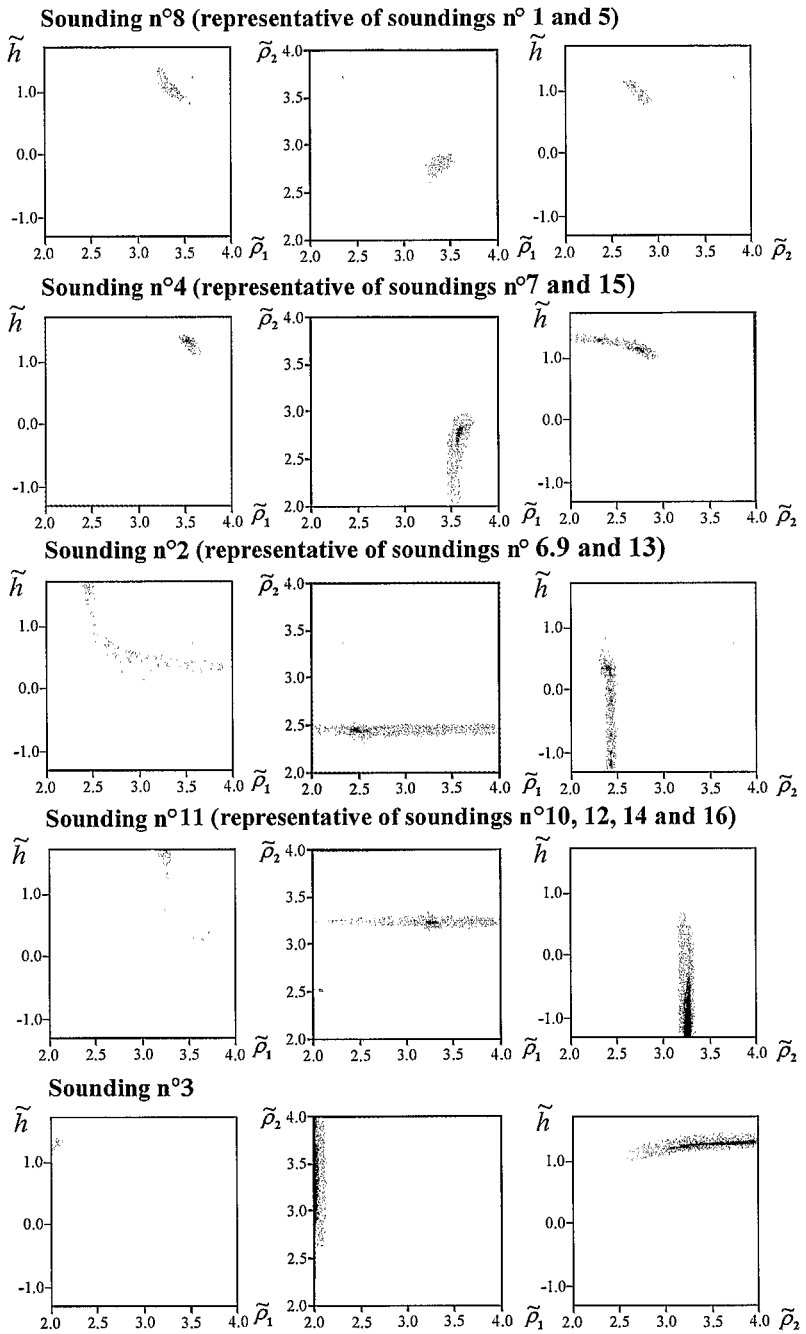

Fig. 9. Nsimi site: results of Bayesian inversion; representation of probability density for representative soundings. $\log(\rho_1)$ versus $\log(h)$ (left), $\log(\rho_1)$ versus $\log(\rho_2)$ (centre) and $\log(\rho_2)$ versus $\log(h)$ (right).

computer, seems unreasonable. It is therefore clear that the Bayesian approach can only be used with a limited number of parameters.

Anyway, since the data were already available, TPM Bayesian approach could also be tested even (or particularly) if the site characteristics are less favourable than for the first case history presented. We only used the three Wenner maps corresponding to one date of the total monitoring and extracted from these maps 16 TPM soundings.

Considering the probability law patterns, the results obtained from the Bayesian inversion were separated into four groups (Fig. 8):

- soundings for which all the parameters are well-determined: sounding nos. 8, 1 and 5.
- soundings for which the PDF lengthens according to r_2, revealing an ambiguity on this parameter: sounding nos. 4, 7 and 15.
- soundings for which the PDF lengthens according to r_1 and h, for which only r_2 is well-determined: sounding nos. 2, 6, 9 and 13 (r_2 about 300 Ω m) and sounding nos. 11, 10, 12, 14 and 16 (r_2 about 1600 Ω m).
- sounding no. 3 for which the exploration domain for r_1 has not been set large enough to get all possibilities.

These four groups of results provide a good insight on what can be encountered on real field conditions: the case for which TPM approach is really suitable and parameters a_0 and k are well-selected (first group), the case for which only the resistivity and the thickness of the first layer are correctly determined (second group), the case for which only the resistivity of the second layer is correctly determined (third group), and the case for which the a priori range of resistivity fixed for the Bayesian inversion is not suitable (fourth group).

The third group is particularly interesting. The simplified pseudosections presented on Fig. 8 show that for the soundings belonging to this group, there is no clear layering. The first subgroup only presents the resistive layer and the second subgroup, only the conductive layer. Hence, if we assume that a two-layer model is suitable, the first subgroup could correspond to points where the resistive first layer is too thick to investigate the conductive second layer with the chosen TMP parameters. On the contrary, the second subgroup could correspond to points where the resistive first layer is too thin to have an influence on the measured apparent resistivities. It should be noted that in both cases, the prominent layer is considered as the second layer by the Bayesian inversion. Meanwhile, the results of the Bayesian inversion and the presentation density for representative soundings are shown in Fig. 9.

These examples still illustrate the advantages of the Bayesian inversion with respect to other classical inversion methods. The most important point is that the result brings a quantified description of all ambiguities included in the model used for the interpretation of the measurements but it should also be pointed out that a two-layer model may not be suitable to describe properly the actual structure of the ground influencing the apparent resistivity data. In this case, TPM results should be considered with a lot of precaution.

4. Conclusion

A quick electrical sounding method, consisting of only three measurements of apparent resistivity, the so-called Three-Point method (TPM), is sufficient under certain conditions to calculate the parameters of a two-layer model. Traditional inversion methods provide a solution to such a limited data set but may not provide any information on the reliability of this solution. Indeed, even if a quantitative analysis is performed, it is of limited use because of the lack of information on all possible equivalent solutions compatible with the data. Both synthetic and field data show that the use of a Bayesian inversion method permits us to describe all the solutions in terms of probabilities. On one hand, this probabilistic method gives valuable information on the relevance of TPM. It particularly allows to choose accurately the optimal increase of electrode separations. On the other hand, and this is the most significant result, the Bayesian inversion method appears to be a very efficient tool to take benefits from limited data set.

Finally, TPM plus Bayesian inversion approaches appear to be a powerful unbiased tool that allows reliable interpolation between sparse complete elec-

trical soundings. Indeed, it allows a rapid field survey over a fine mesh and provides a valuable quantification of interpolation quality.

References

Barker, R.D., 1992. A simple algorithm for electrical imaging of the subsurface. First Break 10, 53–62.

Bhattacharya, B.K., Patra, H.P., 1968. Direct Current Geoelectric Sounding Principles and Interpretation. Elsevier, Amsterdam, 135 pp.

Chambers, J., Ogilvy, R., Meldrum, P., Nissen, J., 1999. 3D resistivity imaging of buried oil and tar-contaminated waste deposit. Eur. J. Environ. Eng. Geophys. 4 (1), 3–14.

Dabas, M., Tabbagh, A., Tabbagh, J., 1994. 3-D inversion in subsurface electrical surveying: I. Theory. Geophys. J. Int. 119, 975–990.

Edwards, L.S., 1977. A modified pseudosection for resistivity and induced-polarization. Geophysics 42, 1020–1036.

Florsch, N., Hinderer, J., 2000. Bayesian estimation of the free core nutation parameters from the analysis of precise tidal gravity data. Phys. Earth Planet. Inter. 117, 21–35.

Griffiths, D.H., Barker, R.D., 1993. Two-dimensional resistivity imaging and modelling in areas of complex geology. J. Appl. Geophys. 29, 211–226.

Griffiths, D.H., Turnbull, J., 1985. A multi-electrode array for resistivity surveying. First Break 3, 16–20.

Griffiths, D.H., Turnbull, J., Olayinka, A.I., 1990. Two-dimensional resistivity mapping with a computer-controlled array. First Break 8, 121–129.

Koefed, O., 1979. Geosounding Principles: 1. Resistivity Sounding Measurements. Elsevier, Amsterdam, 276 pp.

Kunetz, G., 1966. Principles of direct current resistivity prospecting. Geoexploration Monographs Ser. 1, No. 1, 103 pp.

Lokhe, M.H., Barker, R.D., 1996a. Rapid least square inversion of apparent resistivity pseudosections by a quasi-Newton method. Geophys. Prospect., 44, Borntraeger Ed., Berlin, pp. 131–152.

Lokhe, M.H., Barker, R.D., 1996b. Practical techniques for 3-D resistivity surveys and data inversion. Geophys. Prospect. 44, 499–523.

Olivia, P., Viers, J., Dupré, B., Fortuné, P., Martin, F., Braun, J.J., Nahon, D., Robain, H., 1999. The effect of organic matter on chemical weathering: study of a small tropical watershed: Nsimi–Zoétélé site, Cameroon. Geochim. Cosmochim. Acta 63 (23–24), 4013–4035.

Olivié-Lauquet, G., Allard, T., Benedetti, M., Muller, J.-P., 1999. Chemical distribution of trivalent iron in riverine material from a tropical ecosystem. Water Res. 33 (11), 2726–2736 (Oxford).

Park, S., 1998. Fluid migration in the vadose zone from 3-D inversion of resistivity monitoring data. Geophysics 63, 41–51.

Press, W.H., Teukolsky, S.A., Vetterling, W.T., Flannery, B.P., 1996. Numerical recipes in FORTRAN 90. The Art of Parallel Computing. 2nd edn. Cambridge Univ. Press, London, 576 pp.

Ritz, M., Robain, H., Pervago, E., Albouy, Y., Camerlynck, C., Descloitres, M., Mariko, A., 1999. Improvement to resistivity pseudosection modelling by removal of near surface inhomogeneity effects: application to a soil system of southern Cameroon. Geophys. Prospect. 47, 85–101.

Robain, H., Albouy, Y., Braun, J.J., Ndam, J.R., 1995. An electrical monitoring of an elementary watershed in the rain forest of Cameroon. Proceedings of Environmental and Engineering Geophysics, 25–27/09/1995. G. Ranieri Ed., Torino, pp. 411–414.

Robain, H., Descloitres, M., Ritz, M., Yéné Atangana, Q., 1996. A multiscale electrical survey of a lateritical soil system in African rain forest. J. Appl. Geophys. 34, 237–253.

Robain, H., Albouy, Y., Camerlynck, C., Dabas, M., Descloitres, M., Tabbagh, A., 1998. Geophysical surveys contribution to structural and behavioural knowledge of tropical soils. Application to mapping purpose. Proceedings of World Congress of Soil Science, AISS, Montpellier 20–26/08/1998: Symposium 17, Registration 1217. CIRAD Ed.

Roy, A., Apparao, A., 1971. Depth of investigation in direct current methods. Geophysics 36, 943–959.

Sasaki, Y., 1994. 3-D resistivity inversion using the finite element method. Geophysics 59, 1839–1848.

Scollar, I., Tabbagh, A., Hesse, A., Herzog, I., 1990. Topics in remote sensing 2. Archeological Prospecting and Remote Sensing. Cambridge Univ. Press, London, 674 pp.

Tarantola, A., Valette, B., 1982a. Generalized nonlinear inverse problems solved using the least square criterion. Rev. Geophys. Space Phys. 20 (2), 219–232.

Tarantola, A., Valette, B., 1982b. Inverse problems—quest for information. J. Geophys. 50, 159–170.

Tarentola, A., 1987. Inverse problem theory. Methods for Data Fitting and Model Parameter Estimation. Elsevier, Amsterdam, 614 pp.

Telford, W.M., Geldart, L.P., Sheriff, R.E., 1990. Applied Geophysics. 2nd edn. Cambridge Univ. Press, London, 770 pp.

Viers, J., Dupré, B., Polvé, M., Schott, J., Dandurand, J.L., Braun, J.J., 1997. Chemical weathering in the drainage basin of a tropical watershed (Nsimi–Zoetele site, Cameroon): comparison between organic-poor and organic-rich waters. Chem. Geol. 163, 181–206.

Zhang, J., Rodi, W., Mackie, R.L., Shi, W., 1995. 3-D resistivity forward modelling and inversion using conjugate gradients. Geophysics 60, 1313–1325.